

Dissipative dynamics of interacting quantal degrees of freedom in spherical nuclei

E. S. Hernández*

Consejo Nacional de Investigaciones Científicas y Técnicas, Buenos Aires, Argentina

C. O. Dorso

*Departamento de Física, Facultad de Ciencias Exactas y Naturales, Universidad de Buenos Aires,
1428 Buenos Aires, Argentina*

(Received 1 November 1983)

A model of quantal Brownian motion in fermionic reservoirs is applied to study the time evolution of a giant isovector dipole mode in ^{208}Pb . The coupled equations of irreversible motion for the excited collective mode and for the nucleon intrinsic degrees of freedom are simultaneously solved and their energies, entropies, and relative populations are observed over a lengthy time interval. The resonant decay can be seen together with the excitation of the Fermi sea towards a non-Fermi asymptotic distribution. It is found that the effective decay rate is smaller than the downwards transition rate, in contrast to the widespread assumption in microscopic models of resonance damping. Diffusion, as well as dissipation, appears as a feature of mutual equilibration.

I. INTRODUCTION

Since the origins of nuclear theory, collective and single-particle motion have been regarded as complementary, nonexclusive aspects of a very complicated dynamics involving many degrees of freedom. Presently, the delicate correlations between both profiles of the twofolded subject are being examined with renewed enthusiasm.¹⁻⁴ Due to the possibility of observing, with the probe of heavy ion reactions,^{5,6} the transfer of large amounts of energy, mass, and angular momentum over finite time intervals, most efforts in the above-mentioned direction have been oriented towards establishing dissipation mechanisms in large amplitude collective motion. However, after the pioneering attempts to describe transport processes in the nuclear fluid within theoretical frames that involve almost stationary intrinsic degrees of freedom,^{5,6} interest has drifted towards the mutual influence of either type of excitation on the other one. In such a spirit, Mukamel *et al.*¹ study the interplay between collective and stochastic excitations regarding both in the same footing, namely allowing for the time evolution of the fermionic coordinates. Similarly, Takigawa *et al.*² derive a master equation for the nucleonic reservoir coupled to the collective motion through a stochastic Hamiltonian in a frame that resembles the linear response theory.⁷ More recently, Ayik and Nörenberg³ utilize projection techniques⁸ to examine the decay of a Slater determinant of single-particle (s.p.) states into more complex configurations due to coupling with macroscopic motion in a nuclear system. In this case, the evolution of the Fermi liquid is driven by a masterlike equation rather than by a kinetic, quantal Boltzmann equation.

These studies coincide in the consideration of either large amplitude or low frequency collective motion that can be regarded as classical in the lowest approximation. It is not clear that substantially quantal, high-frequency modes like giant resonances in nuclei could be straightfor-

wardly described resorting to these theories, especially if one is interested in predicting the major evidence of irreversible coupling between collective and intrinsic degrees of freedom, namely the damping width. A detailed analysis of the origin and structure of the damping resonance width has been recently given by Wambach *et al.*,⁴ whose approach lies on similar grounds as those in Refs. 1-3 since both the macroscopic and the microscopic systems are simultaneously dealt with in the framework of Green's function theory.

In a previous paper,⁹ we have presented a model that conjugates features of the above-mentioned views in the following sense. A quantal, high-frequency oscillation—rather than a low-energy surface vibration, or the slow relative motion between two heavy ions—in the nuclear environment, aimed at representing an isospin density wave,¹⁰ an elastic vibration,¹¹ or a zero-sound mode¹² is supposed to couple to the fermionic motion through a residual particle-phonon interaction. Appropriate utilization of either reducing^{13,14} or projection^{8,13} techniques, of current use in nonequilibrium statistical mechanics, with a minimum of simplifying working hypotheses—the major one being the weak-coupling assumption—allows us to extract from the Liouville-von Neumann equation a set of evolution laws for the coupled dynamics of the subsystems. While the density matrix describing the population of the oscillator spectrum obeys a quantal equation with microscopically derived transition rates, the fermionic reservoir evolves according to a modified kinetic equation. Equilibration is then irreversibly driven by the mutual coupling. In Ref. 9, a solvable model has been worked out and it has been proven that an asymptotic lifetime, or inverse damping width, can be extracted for the collective mode as one follows the time evolution of its density matrix. Furthermore, estimates of the s.p. damping width contributed by such a coupling have been given in Ref. 15 for a regime of nuclear temperature and collective energy resembling that expected in the vicinity of the isovector

giant dipole resonance (GDR) in ^{208}Pb .

This presentation differs from the work of other authors¹⁶ who face the prediction of the collective damping width by examining the peaks of the response function in the time-independent framework of linear response theory^{17,18} in the choice of the coupling mechanism. The latter is here explicitly attributed to the residual particle-phonon interaction⁹ rather than to the force exerted by an exciting external field as in Ref. 16. However, we are building our collective excitation on an unperturbed, normal Fermi sea, instead of a superconducting ground state like that chosen by Jensen *et al.* in their analysis of pairing and quadrupole vibration spread in ^{238}U .

In the present work we show that the major model restrictions in these prior works^{9,15} can be released. The equations of irreversible evolution, adequately modified in order to describe a rotationally invariant object such as a finite nucleus, provide useful and original information concerning resonance decay in nuclei. As an example, the isovector GDR in ^{208}Pb is followed during its decay over a finite time length. The Fermi sea, set at the origin of time at a stationary state, becomes disturbed when sudden excitation of the mode to which it couples takes place. The progress of the fermionic excitation can be followed as well. As a by-product of these observations, a figure for the resonance width can be extracted and defined up to an energy factor associated with a typical interaction strength.

This paper is organized as follows. In Sec. II we present the formulae to be numerically integrated; no derivation is given here and we refer the reader to Refs. 9 and 15. We rather specify in this section the details intrinsic to the particular system we are attempting to describe. In Sec. III, we discuss the range of the approximations established in the original theory and the arguments to relax them when needed. The calculations here undertaken are described in this section. The results are discussed in Sec. IV, while the conclusions and perspectives in this field are summarized in Sec. V.

II. THE EQUATIONS OF IRREVERSIBLE DYNAMICS IN THE SPHERICAL BASIS

In this section we present an abridged version of the genesis of the dynamical equations for the system under

$$\begin{aligned}
 V &= \sum_{\alpha\mu qM} \lambda_{\alpha\mu}^{qM} \Gamma_{TJ\pi}^{qM\dagger} [b_{\mu}^{\dagger} b_{\alpha}]^{TJ\pi} + \text{H.c.} \\
 &= \sum_{\alpha\mu qM} \lambda_{\alpha\mu}^{qM} \langle j_{\alpha} m_{\alpha} j_{\mu} m_{\mu} | j_{\alpha} j_{\mu} JM \rangle \langle \frac{1}{2} \tau_{\alpha} \frac{1}{2} \tau_{\mu} | \frac{1}{2} \frac{1}{2} T_q \rangle \frac{1 + (-)^{l_{\alpha} + l_{\mu} + \pi}}{2} \Gamma_{TJ\pi}^{qM\dagger} b_{\mu}^{\dagger} b_{\alpha} + \text{H.c.}
 \end{aligned} \tag{2.6}$$

In this expression, $\lambda_{\alpha\mu}^{qM}$ is an interaction matrix element and the s.p. labels A show up in two specified categories,^{9,15} according to their particle (α, β, \dots) or hole (μ, ν, \dots) nature.

Once the representation of the interaction has been established, it is easy to reproduce the calculation steps leading to the coupled equations of motion, namely the master equation for the Liouville state vector of the collective mode⁹ and the modified kinetic equation for the fermion density matrix.^{9,15} In the present framework, they take the form (hereafter we drop the $TJ\pi$ labels that will remain widely understood),

$$\dot{\rho}_n^{qM} = W_+^{qM} (\rho_{n+1}^{qM} - \rho_n^{qM}) + W_-^{qM} (\rho_{n-1}^{qM} - \rho_n^{qM}), \tag{2.7a}$$

consideration. Since enough room for details of the general formulation has been allowed in previous papers^{9,15} (also see Refs. 13 and 19), we will just outline the road towards these equations when the fermionic reservoir or heat bath is a spherical nucleus, rather than extensive nuclear matter. Let $\rho_{TJ\pi}$ be the observed (i.e., asymptotic) density matrix for a harmonic collective mode labeled by isospin T , total angular momentum J , and parity π ,

$$\rho_{TJ\pi} = \sum_{q=\pm 1} \sum_{M=-J}^J \sum_n \rho_{TJ\pi n}^{qM} |nqM; TJ\pi\rangle \langle nqM; TJ\pi|. \tag{2.1}$$

Here q denotes the isospin character of the collective oscillation, namely $q=1$ for protons and $q=-1$ for neutrons. The label n indicates the number of oscillator quanta for given q and M , or

$$|nqM; TJ\pi\rangle \approx (\Gamma_{TJ\pi}^{\dagger qM})^n |0qM; TJ\pi\rangle, \tag{2.2}$$

where $|0qM; TJ\pi\rangle$ is the vacuum for the class of phonons created by the boson operator $\Gamma_{TJ\pi}^{\dagger qM}$.

Similarly, let $\rho(1)$ be the reduced one-fermion density matrix in a s.p. basis $|A\rangle = |\tau_A N_A j_A l_A\rangle$, where $\tau_A = \frac{1}{2}$ ($-\frac{1}{2}$) for protons (neutrons);

$$\rho(1) = \sum_A \sum_{m_A=-j_A}^{j_A} \rho_A^{m_A} |m_A; A\rangle \langle m_A; A|. \tag{2.3}$$

In this scheme, the total population of an oscillator state with n quanta is

$$\rho_n = \sum_{q,M} \rho_{TJ\pi,n}^{qM}, \tag{2.4}$$

while the total population of a s.p. orbital $|A\rangle$ is

$$\rho_A = \sum_{m_A} \rho_A^{m_A}. \tag{2.5}$$

We assume that the interaction between the bosonic and fermionic subsystems into which we are splitting our nucleus can be represented by a standard particle-phonon interaction,

$$\begin{aligned} \dot{\rho}_A^{m_A} = & (B^{qM} - \rho_0^{qM}) \left[\sum_{\mu, m_\mu} |\lambda_{\alpha\mu}^{qM}|^2 \mathcal{F}^{qM}(\epsilon_{A\mu}) \rho_\mu^{m_\mu} (1 - \rho_A^{m_A}) - \sum_{\alpha, m_\alpha} |\lambda_{\alpha A}^{qM}|^2 \mathcal{F}^{qM}(\epsilon_{\alpha A}) \rho_A^{m_A} (1 - \rho_\alpha^{m_\alpha}) \right] \\ & + (B^{qM} - \rho_N^{qM}) \left[\sum_{\alpha, m_\alpha} |\lambda_{\alpha A}^{qM}|^2 \mathcal{F}^{qM}(\epsilon_{\alpha A}) \rho_\alpha^{m_\alpha} (1 - \rho_A^{m_A}) - \sum_{\mu, m_\mu} |\lambda_{A\mu}^{qM}|^2 \mathcal{F}^{qM}(\epsilon_{A\mu}) \rho_A^{m_A} (1 - \rho_\mu^{m_\mu}) \right] + \dot{\rho}_A^{m_A}(\text{kin}), \end{aligned} \quad (2.7b)$$

where the symbols to be explained are the following:

(i) the transition rates W_{\pm}^{qM} for each kind of nucleon and spin projection,

$$W_{+}^{qM} = \sum_{\alpha\mu m_\alpha m_\mu} |\lambda_{\alpha\mu}^{qM}|^2 \mathcal{F}^{qM}(\epsilon_{\alpha\mu}) \rho_\mu^{m_\mu} (1 - \rho_\alpha^{m_\alpha}), \quad (2.8a)$$

$$W_{-}^{qM} = \sum_{\alpha\mu m_\alpha m_\mu} |\lambda_{\alpha\mu}^{qM}|^2 \mathcal{F}^{qM}(\epsilon_{\alpha\mu}) \rho_\alpha^{m_\alpha} (1 - \rho_\mu^{m_\mu}); \quad (2.8b)$$

(ii) the energy-spin-isospin form factor,

$$\begin{aligned} \mathcal{F}^{qM}(\epsilon_{\alpha\mu}) = & F(\epsilon_{\alpha\mu}) \langle j_\alpha m_\alpha j_\mu m_\mu | j_\alpha j_\mu TM \rangle^2 \\ & \times \langle \frac{1}{2} \tau_\alpha \frac{1}{2} \tau_\mu | \frac{1}{2} Tq \rangle^2, \end{aligned} \quad (2.9)$$

where $F(\epsilon_{\alpha\mu})$ is the filter associated with nonstrict energy conservation,^{9,15} usually taking the Lorentzian shape;

(iii) the boson normalization factor B^{qM} to be specified below;

(iv) the kinetic collisional derivative $\dot{\rho}_A^{m_A}(\text{kin})$, associated with the residual two-particle collisions.

These equations possess the following characteristics. First, they describe the evolution in a given subspace labeled by q and M , different subspaces remaining dynamically uncoupled. Of course, each value of q is in correspondence with the s.p. isospin τ_A associated with the label A in Eqs. (2.7b). In other words, these equations govern the motion of either proton or neutron harmonic oscillations of given spin, spin projection, and parity. Second, the normalization of the density matrices is strictly conserved in each subspace. This means that

$$\sum_n \rho_n^{qM} = B^{qM}, \quad (2.10a)$$

$$\sum_{A, m_A} \rho_A^{m_A} = F^{qM}, \quad (2.10b)$$

where B and F stand for constants associated with bosonic and fermionic degrees of freedom, respectively, whose values can be fixed as follows. Let us observe that the boson density is normalized as

$$\begin{aligned} 1 = & \sum_{q=\pm 1} \sum_{M=-J}^J \sum_n \rho_n^{qM} \\ = & \sum_{q=\pm 1} \sum_{M=-J}^J B^{qM} \\ = & B^+ + B^-, \end{aligned} \quad (2.11)$$

where we have defined

$$B^q = \sum_{M=-J}^J B^{qM}. \quad (2.12)$$

These constants can be specified if we consider that at $t=0$ the oscillator lies in its unperturbed ground state and the spatial pattern is spherically symmetric. Thus, Eqs. (2.12) are characterized by an average $\overline{B^{qM}} = b^q$, so that

$$B^q = (2J+1)b^q. \quad (2.13)$$

We assume that the relative weights of B^\pm are, respectively, proportional to the total numbers of proton and neutron pairs satisfying the total spin and parity selection rules, namely

$$B^q = \frac{J^q}{J^q + J^{-q}}. \quad (2.14)$$

From (2.12) to (2.14) we obtain, for any q and M ,

$$b^q = \overline{B^{qM}} = \frac{1}{2J+1} \frac{J^q}{J^q + J^{-q}}. \quad (2.15)$$

With respect to the fermion normalization factors, we simply introduce the spherical symmetry argument and notice that

$$\overline{F^{+M}} = Z/(2J+1), \quad (2.16a)$$

$$\overline{F^{-M}} = N/(2J+1). \quad (2.16b)$$

Finally, it should be stressed that the dynamics contained in Eqs. (2.7) is a causal one, leading to asymptotic equilibration by means of the residual interaction between the competing systems. Equilibrium is achieved when gain and loss contributions—in other words, when the rates of population and depopulation, respectively, of a given unperturbed level of either subsystem—balance each other. Any nonvanishing difference between these two rates gives rise to a finite collisional derivative, in charge of bringing equilibration back into the system.

As a final word of caution for this section, we must remind the reader that the microscopic particle-hole structure of the transferred phonons has not been explicitly considered. The underlying picture can be regarded as that of a quantal multipole harmonic oscillator performing Brownian motion in a spherical cavity. At the present stage of the theoretical development there is no way of overcoming this limitation at a relatively low cost. However, we will see in the next sections that the most relevant features of resonance damping are contained in this simple framework, since a phenomenological renormalization of the transition rates that takes care of Pauli blocking effects, utilizing strength functions from random-phase-approximation (RPA) calculations, does not give significant deviations from the Pauli-violating description provided by Eqs. (2.7).

III. APPLICATION TO THE ISOVECTOR GIANT DIPOLE RESONANCE IN ^{208}Pb

As an application of the theory presented in Sec. II, we design a simplified model for a resonant isovector dipole mode in ^{208}Pb . The s.p. spectrum is that used in Ref. 20 and the experimental resonant energy is²¹ $\hbar\Omega = 13.8$ MeV. The coupling matrix elements $\lambda_{\alpha\mu}$ are set identically equal to the unity; the constant λ is otherwise a time or energy scaling factor that can be either fit to experimental data or given a microscopic ansatz (see, for example, Ref. 22).

At this point a question could be raised regarding the legitimacy of the use of kinetic methods to compute the evolution of a system with both discrete and finite spectra. We must keep in mind that these two characteristics possess a different origin. The discreteness arises from the fact that s.p. energies and orbitals are determined in a fashion that involves mostly stationary or quasistationary behavior, for instance, via spectroscopic measurements. In fact, a many-body system with residual and finite range two-body interactions does not exhibit a discrete spectrum of s.p. excitations, but rather a continuum generated by overlapping broadened levels. Notice that we are dismissing the unbound portion of the s.p. spectrum, since we are interested in the damping width, rather than in the escape width that is usually a small fraction of the total broadening.⁴ By contrast, the finite spectrum arises from a calculational need. As will be later seen when discussing the numerical results, the truncation of the model space does not represent a significant limitation, since (i) as in standard shell model calculations, suppression of the highly excited part of the spectrum is valid to the extent to which the transition rates to those levels are negligible within the dominant scale; (ii) the processes we study here are weighted by an energy form factor [see Eq. (2.9)] that further privileges transitions within a selected band and dampens away the high lying spectrum.

In the present work the most interesting effect related to the existence of both particle-particle and particle-phonon residual interactions is the possibility of assigning a finite lifetime to the collisional operator^{9,13-15,19} that gives rise to the right-hand side of Eqs. (2.7). This fact is reflected in the broad energy form factor $F(\epsilon_{\alpha\mu})$ of the

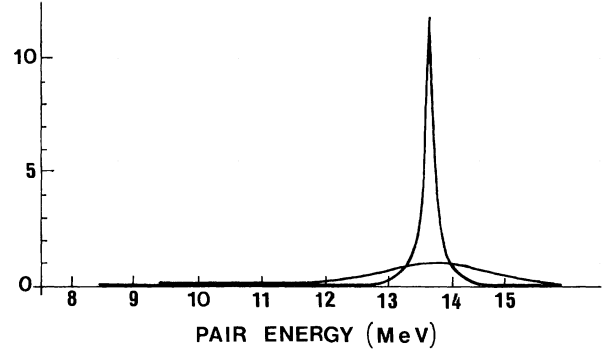


FIG. 1. The energy Lorentzian form factor $F(\epsilon_{\alpha\mu})$ as a function of the pair energy (in MeV) for different width parameters $\hbar\gamma$. The center of the filter lies at the phonon energy $\hbar\Omega = 13.8$ MeV.

Lorentzian-type [Eq. (2.9)] centered at the phonon energy $\hbar\Omega$. The magnitude of the energy width $\hbar\gamma$ in $F(\epsilon_{\alpha\mu})$, where

$$F(\epsilon_{\alpha\mu}) = \frac{\hbar\gamma}{(\epsilon_{\alpha\mu} - \hbar\Omega)^2 + (\hbar\gamma)^2}, \quad (3.1)$$

should be selected with some caution in view of its significance. Let us recall that the characteristic lifetimes of our subsystems are related to the following: (i) s.p. level broadening and collective level broadening, both due to the mutual interaction, and (ii) s.p. level broadening which originated in the two-fermion residual interaction. However, γ^{-1} is a collisional lifetime, in other words, it is a correlation time τ_c that represents the duration of an unobserved particle-phonon collision and is consequently related to its interaction range. This is essentially a microscopic parameter and is thus substantially different from the macroscopic broadenings enumerated above, that already bear the effect of averaging with respect to unobserved degrees of freedom. The point to be stressed here is that, although both individual fermion and boson lifetimes originate in their microscopic coupling that takes place within a correlation time $\tau_c = \gamma^{-1}$, the measurable consequence of the interaction is an average relaxation

TABLE I. The relative weight L_i assigned by the Lorentzian energy form factor of the pair states $(\alpha\mu)$ with pair energy $\omega_{\alpha\mu}$ closest to the phonon energy $\hbar\Omega$ normalized with respect to the most favored transition $i = 1$.

i	$(\alpha\mu)$	$\omega_{\alpha\mu}$ (MeV)	$\hbar\gamma = 0.1$ MeV		$\hbar\gamma = 1$ MeV		$\hbar\gamma = 10$ MeV	
			L_i	L_i/L_{i+1}	L_i	L_i/L_{i+1}	L_i	L_i/L_{i+1}
1	(p 2 $f_{7/2}$ p 1 $g_{9/2}$)	12.56	1.0		1.0		1.0	
2	(p 1 $h_{9/2}$ p 1 $g_{9/2}$)	11.6	0.337	2.967	0.454	2.203	0.965	1.036
3	(p 2 $f_{5/2}$ p 1 $g_{7/2}$)	10.96	0.192	1.755	0.280	1.621	0.935	1.032
4	(n 2 $g_{7/2}$ n 1 $h_{9/2}$)	9.4	0.080	2.4	0.125	2.24	0.850	1.1
5	(p 2 $f_{5/2}$ p 2 $d_{5/2}$)	9.23	0.074	1.081	0.116	1.078	0.840	1.012
6	(p 3 $g_{3/2}$ p 2 $d_{5/2}$)	8.75	0.061	1.213	0.096	1.208	0.819	1.026

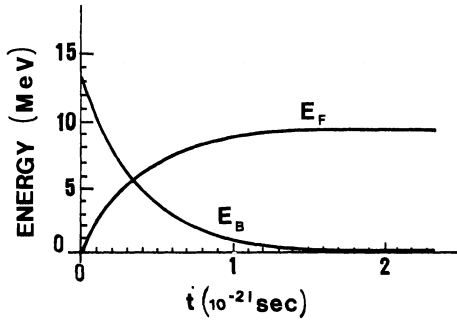


FIG. 2. The boson and fermion energies E_B and E_F , respectively, as functions of time. It is assumed that at $t=0$, the oscillator level $n=1$ is populated, the rest of the spectrum being depleted, while the nucleons distribute in an unperturbed Fermi sea. The width of the energy filter is $\hbar\gamma=1$ MeV and the phonon energy is $\hbar\Omega=13.8$ MeV.

time, larger than τ_c , associated with the inverse level width. Since we actually ignore the magnitude of τ_c , we are forced to regard either it or γ as parameters whose influence on the numerical results has to be examined.

In order to illustrate the theory in Sec. II and the above considerations in the case of the giant $T=1, J^\pi=1^-$ mode in ^{208}Pb , we have numerically solved Eqs. (2.7) for a variety of situations labeled by different values of the Lorentzian width $\hbar\gamma$. It should be noted that since we are dealing with energy nonconserving (inelastic) scattering events, the total energy of the combined system is not a constant of the motion. The amount of nonconservation is measured by the size of $\hbar\gamma$, i.e.,

$$|\dot{E}_B - \dot{E}_F| \approx \hbar\Omega\gamma. \quad (3.2)$$

Our criterion for a choice of γ is based on the smallest energy fluctuation. It has been seen that the quantity $|\dot{E}_B - \dot{E}_F|$ saturates for the value $\hbar\gamma \sim 0.1$ MeV; smaller figures for this parameter do not improve energy conservation. This is due to the fact that for the current choice of s.p. spectrum, a Lorentzian width of 0.1 MeV not only excludes all pair levels ($\alpha\mu$) from the vicinity of the peak at 13.8 MeV, but the relative weight assigned to every allowed transition remains almost constant when $\hbar\gamma$ diminishes. This is illustrated in Fig. 1, where Lorentzian functions are drawn for $\hbar\gamma=10, 1$, and 0.1 MeV. The pair spectrum $\omega_{\alpha\mu}$ is indicated on the abscissa axis. The rela-

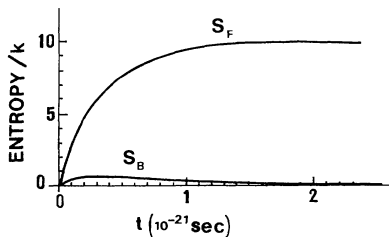


FIG. 3. The boson and fermion entropies S_B and S_F , respectively, in units of the Boltzmann constant $k=8.62 \times 10^{-11}$ MeV $^\circ\text{K}^{-1}$ as functions of time. The details are the same as in Fig. 2.

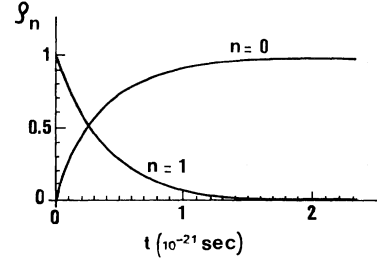


FIG. 4. The oscillator occupation numbers $\rho_0(t)$ and $\rho_1(t)$, with the same conditions of Figs. 2 and 3.

tive weights for those levels with energies closest to $\hbar\Omega$ are shown in Table I, where the saturation effect is clearly displayed.

Figures 2–7 exhibit the following calculations, corresponding to the case $\hbar\gamma=1$ MeV, as functions of time (in units 10^{-21} sec). The boson and fermion energies, the corresponding entropies, and the occupation of the oscillator ground state and the first excited level are shown, respectively, in Figs. 2, 3, and 4. The energy logarithmic derivative,

$$\nu_E(t) = \frac{\dot{E}_B(t)}{E_B(t) - E_B(\infty)}, \quad (3.3)$$

is displayed in Fig. 5 together with the average transition rates

$$\overline{W}^+ = \frac{1}{2(2J+1)} \sum_{qM} W^{+qM}. \quad (3.4)$$

In Fig. 6, we show pictures of the time evolution of the relative variation of the fermion population,

$$\delta\rho_A(t) = \frac{\rho_A(t) - \rho_A(0)}{\rho_A(0)}, \quad (3.5)$$

taken every 2.85×10^{-21} sec. We remark that the time step in our calculations has been taken as 0.057×10^{-21} sec. For t larger than the highest time in the figure ($t_{\text{max}} = 17.1 \times 10^{-21}$ sec) saturation of the population pattern is graphically achieved in the current scale. Finally, in Fig. 7 the final fermionic variations $\delta\rho_A(\infty)$ are displayed.

In these calculations, the intrinsic fermion collisional derivative $\dot{\rho}_{\text{kin}}$ has been set equal to zero, since it has been seen in Ref. 15 that its contribution is relevant for s.p. lev-

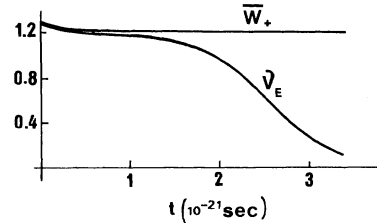


FIG. 5. The logarithmic derivative of the boson energy (absolute value) and the average downwards transition rate for the collective mode as functions of time. The details are the same as in Figs. 2–4.

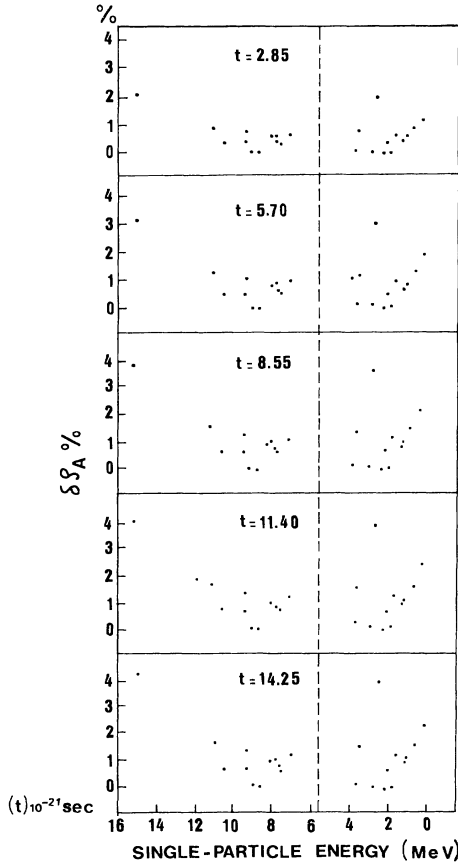


FIG. 6. The time evolution of the Fermi sea. Relative variations $\delta\rho_A$ of the fermion population, defined in Eq. (3.5), are displayed against the single-particle energy ϵ_A (in MeV) for the indicated instants. Details are the same as in Figs. 2–5.

els lying more than a tenth of an MeV above the Fermi level. The dimension of the numerical problem has been cut off by a factor of 2 with the approximations

$$\rho_n^{qM} \approx B^q \rho_n^M, \quad (3.6a)$$

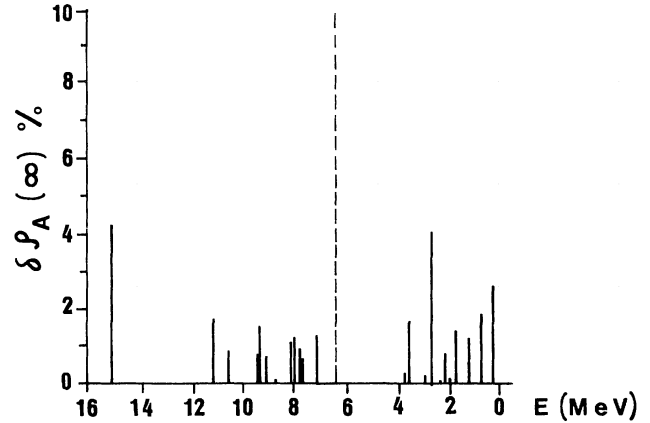


FIG. 7. The equilibrated fermion population for $t = \infty$. This represents the final picture in Fig. 6, arising as a long-time run.

$$W_+^{qM} \approx B^q W_+^M, \quad (3.6b)$$

$$B^q \approx \frac{1}{2}. \quad (3.7)$$

This is a reasonable guess for heavy systems and holds to below 1% in the case of ^{208}Pb . All frequencies and transition rates are given in $10^{21} \text{ sec}^{-1} |\lambda|^2$, where λ is given in MeV. The normalization of both fermion and boson densities is strictly conserved throughout the whole time evolution. Furthermore, since these computations represent a structureless harmonic oscillator coupled to a spherical fermionic environment, a question that naturally arises concerns the influence of the microscopic constitution of the collective phonon in the proposed dynamics. From the simplest minded point of view, an estimate of such an effect can be given if one refers to the well-established random-phase-approximation (RPA) description of the dipole phonon in ^{208}Pb (see, for example, Ref. 4) and to its corresponding strength function. We have assigned to the pair level spectrum a probability weight $P_{\alpha\mu}$ constructed

TABLE II. The asymptotic relative variation of the fermion population $\delta\rho_A(t)$, evaluated both without and with the Fermi blocking factor $P_{\alpha\mu}$ originated in the structure of the phonon (columns labeled 1 and 2, respectively, for every considered time). The symbols p and n in the left column indicate proton and neutron states, respectively. The single-particle levels are ordered according to increasing energy with respect to an arbitrary although common origin.

A	$t = 2.85 \times 10^{-21} \text{ sec}$		$t = 8.55 \times 10^{-21} \text{ sec}$		$t = \infty$	
	1	2	1	2	1	2
p 1 $g_{9/2}$	2.4	2.1	4.0	3.7	4.4	4.2
p 2 $d_{5/2}$	0.7	0.7	1.2	1.3	1.4	1.4
p 2 $d_{3/2}$	0.5	0.5	1.0	1.0	1.0	1.1
n 3 $p_{1/2}$	0.6	0.6	1.1	1.1	1.2	1.3
p 1 $h_{9/2}$	0.8	0.8	1.4	1.4	1.6	1.7
p 2 $f_{7/2}$	2.3	2.1	3.9	3.6	4.3	4.0
n 3 $d_{5/2}$	0.4	0.4	0.6	0.7	0.7	0.8
n 4 $s_{1/2}$	0.7	0.7	1.1	1.1	1.3	1.4
n 2 $g_{7/2}$	0.5	0.5	0.9	0.9	1.0	1.1
n 3 $d_{3/2}$	0.6	0.6	1.0	1.0	1.1	1.2
p 3 $p_{3/2}$	0.9	0.9	1.5	1.5	1.7	1.8
p 2 $f_{5/2}$	1.3	1.3	2.2	2.2	2.4	2.5

from the strength function in Ref. 4, properly interpolated and normalized. Thus, in our kinetic equation (2.6b) we have accompanied every phonon destruction weight $\rho_\mu(1-\rho_\alpha)$ with $P_{\alpha\mu}$, namely the probability that the pair $(\alpha\mu)$ is present in the coherent oscillation. Correspondingly, the phonon creation events are weighted by the complement $1-P_{\alpha\mu}$. The results for the time evolution of the fermion population and for the final population are shown in Table II.

IV. DISCUSSION OF THE RESULTS

Figures 2–7 contain a complete picture of the combined time evolution of a harmonic mode with $\hbar\Omega=13.8$ MeV and an energy filter with a width $\hbar\gamma=1$ MeV. The energies of the boson and fermion systems (Fig. 2) saturate at the values 0 and 10 MeV, respectively. Since the binding energy of the fermionic reservoir is higher than 1600 MeV, the loss ΔE is lower than 0.2% of the total initial energy. The variation of the entropies (Fig. 3) displays all the features of an H theorem,¹⁴ with the characteristic increase after a finite time and the asymptotic saturation indicating equilibration (remember that absolute values are drawn).

The quanta probabilities $\rho_1(t)$ and $\rho_0(t)$ evolve from unity towards zero and from zero towards unity, respectively (Fig. 4), reflecting the decay of the initial configuration and the population of the unperturbed ground state. Probabilities ρ_n other than ρ_0 and ρ_1 cannot be displayed in the current scale.

In Fig. 5 we can observe an original feature of this model. It is clearly seen that the average transition rate \overline{W}_+ , representing the probability per unit time for phonon destruction transitions, lies higher than the energy logarithmic derivative throughout the whole time interval. This expresses the fact that in the present theory reexcitation processes can be important. The depopulation of the initially excited oscillator level takes place under the complicated dynamics displayed in Eqs. (2.6), where gain-and-loss events dominate the energy transfer. We realize that the time variation of $\overline{W}_+(t)$ is slow enough, thus the evolution can be regarded as adiabatic; this suggests to us the possibility of instantaneously diagonalizing the evolution kernel and assigning the smallest nonvanishing eigenvalue $\lambda_1(t)$ as an instantaneous decay rate for the energy.⁹ In such a case, the eigenvalue contains a contribution from the upwards transition rates W_-^{qM} , as well as from the downwards rates W_+^{qM} associated with the decay of higher populated levels. The presence of high-lying excitations at positive times is a manifestation of the diffusive character of the whole relaxation process. We recognize as well in Fig. 5, three well-defined regions: (a) the large energy transfer taking place in the initial stages of the evolution; (b) the fast slope change in the energy logarithmic derivative; leading to (c) the asymptotic, very small energy transfer associated with the extremely relaxed motion. In this model, the energy broadening of the collective mode is measured by the effective frequency ν_E in the large transfer regime when $E_B(t)$ has dropped to almost $E_B(0)/e$, that for the chosen set of parameters is

close to 1.20 MeV/ $|\lambda|^2$ and lies slightly below the corresponding decay rate \overline{W}_+ .

In Fig. 6 we can appreciate the time evolution of the fermion occupation numbers as functions of the s.p. energy. Relative figures are shown. We realize that the density profiles depart from the Fermi distribution at $t=0$, although in low amounts, not larger than 4%. It is seen that those s.p. states participating in particle-hole transitions with energies close to the resonant energy are privileged with extra population in the course of evolution. In the present case, they are the proton states $(\alpha\mu)=(1g_{9/2}2f_{7/2})$ and $(1g_{9/2}1h_{9/2})$ with transition energies $\hbar\omega_{\alpha\mu}=12.56$ and 11.66 MeV, respectively. The final population is seen in Fig. 7, where the maximum variation corresponds to the proton state $1g_{9/2}$, with $\delta\rho_A \sim 4.4\%$.

Table II displays a comparison between preceding numbers and those reflecting the effect of Pauli blocking induced by the RPA structure of the collective phonon (columns 1 and 2, respectively, for each given time). Only those s.p. states with $\delta\rho_A(t)$ larger than 1% are shown. It is clearly seen that the most significant difference between columns 1 and 2 amounts to 0.3% and corresponds to the privileged proton levels mentioned above. We conclude that for the present set of approximations, the Pauli principle plays no significant role from the quantitative point of view.

V. CONCLUSIONS

In this paper we have shown that the theory of coupled relaxation of quantal macroscopic (harmonic resonant) and nucleonic degrees of freedom can be utilized to study giant resonance decay and excitation of the Fermi sea, from the dynamical viewpoint. For this sake we have numerically solved the quantal master equation for a dipole isovector mode together with the modified kinetic equation for the nucleons in ²⁰⁸Pb. Significant quantities like energy, entropy, and oscillator level population are observed during their time evolution over several time units and the full characteristics of decay towards equilibration are recorded. The examination of the logarithmic derivative of the oscillator energy as time proceeds indicates severe deviations with respect to the average downwards transition rate \overline{W}_+ . Since the latter, taken at the origin of times and evaluated for zero temperature of the heat bath, is the usually adopted figure for the resonance broadening (see, for example, Ref. 4 and references therein), these results indicate the convenience of incorporating reexcitation events into the picture in order to obtain a correct description of collective mode damping. We especially note that the identification of the width with $\overline{W}_+(t=0, T=0)$ is the “never-come-back” approximation²³ which essentially establishes that coherence is destroyed as soon as a particle-hole state in the collective mode excites into a 2p-1h configuration.

This viewpoint due to Danos and Greiner has been further developed by Dover *et al.*,²⁴ who have considered that the giant dipole width can be evaluated as a weighted average of both particle and hole widths, where the latter are provided by optical potential measurements and calcu-

lations. These authors prove in their work that the prediction of collective centroids can be decoupled from the prediction of the spread, coincidentally with the philosophy here adopted, since we have concentrated ourselves on the extraction of damping or lifetime parameters, assuming that the energy location and structure of the collective excitation is given.

It should be noticed that the entropies displayed in Fig. 3 respond to the characteristics of a truly dissipative process, since $S_{\text{total}} = S_B + S_F$ increases towards asymptotic saturation. This is a consequence of the non-Hermitian nature of the generator of the motion in Eqs. (2.7); indeed, the reversible, Schrödinger-type evolution typical of time-dependent Hartree-Fock or random-phase-approximation calculations is overcome in our case by the information loss introduced by the coarse-grained collisional kernel.^{9,15} In this respect, this work contrasts with the very recent presentation of Yannouleas *et al.*,^{25,26} where monotonic energy transfer from a collective mode into other degrees of freedom is achieved in a reversible fashion. Damping in this case—one properly speaks of Landau damping, a well-known process in physics of fluids¹⁴ and quantum liquids²⁷—is associated with a phase mixing type of irreversibility¹⁴ that provides isentropic homogenization in configuration space.

Of course, deeper studies with more accurate selection of parameters and input data are needed before the last word on the subject will be spoken, but to our belief, this model suggests, within its limitations, that attention should be paid to diffusion in the nuclear fluid in addition to dissipation when a particle-phonon interaction is

switched on.

The dynamical framework utilized here also allows one to observe the progress of the excitation of the Fermi sea towards an asymptotic configuration, in which those s.p. states that participate in particle-hole destruction or creation events with transition energies close to resonance are largely favored. The Pauli principle is parametrically enforced through the introduction of the RPA normalized particle-hole strengths into the transition rates; with the current set of parameters and data, no important modifications to the original description are obtained except for slight indications of enhanced nucleon diffusion.

We believe that the present restricted results encourage further work along this line, in view of the various questions posed that cover different facets of the subject, from a systematic study devoted to shed light with respect to the yet free parameters γ and λ , to theoretical refinements aiming at progressive incorporation of other mechanisms of dissipative coupling.

ACKNOWLEDGMENTS

The authors are indebted to the Laboratorio de Física del Plasma at the Universidad de Buenos Aires for access to their computing facilities. One of us (E.S.H.) is grateful to the Consejo Nacional de Investigación Científica y Tecnológica (CONICET), Argentina, for support as a member of the Scientific Research Career. This work was partially supported by Grant No. 9413b/82 from CONICET and by Subsecretaría de Ciencia y Tecnología, Argentina.

*Permanent address: Departamento de Física, Facultad de Ciencias Exactas y Naturales, Universidad de Buenos Aires, 1428 Buenos Aires, Argentina.

¹S. Mukamel, D. H. E. Gross, U. Smilansky, K. Möhring, and M. J. Sobel, *Nucl. Phys.* **A366**, 339 (1981).

²N. Takigawa, K. Niita, Y. Okuhara, and S. Yoshida, *Nucl. Phys.* **A371**, 130 (1981); K. Niita and N. Takigawa, *ibid.* **A397**, 141 (1983).

³S. Ayik and W. Nörenberg, *Z. Phys.* **A 309**, 121 (1982).

⁴J. Wambach, V. K. Mishra, and Li Chu-Hsia, *Nucl. Phys.* **A380**, 285 (1982).

⁵W. Nörenberg and H. A. Weidenmüller, *Introduction to the Theory of Heavy Ion Collisions* (Springer, Berlin, 1976).

⁶L. G. Moretto and R. P. Schmidt, *Rep. Prog. Phys.* **44**, 533 (1981).

⁷H. Hoffmann and P. J. Siemens, *Nucl. Phys.* **A257**, 165 (1976); **A275**, 464 (1977).

⁸S. Nakajima, *Prog. Theor. Phys.* **20**, 948 (1958); R. W. Zwanzig, in *Lectures in Theoretical Physics*, edited by W. S. Brittin, B. W. Downs, and J. Downs (Interscience, New York, 1961).

⁹E. S. Hernández and C. O. Dorso, *Phys. Rev. C* **29**, 1510 (1984).

¹⁰C. Y. Wong, *Phys. Rev. C* **17**, 1832 (1978).

¹¹C. Y. Wong and N. Azziz, *Phys. Rev. C* **24**, 2290 (1981); C. Y. Wong, *ibid.* **25**, 2787 (1982).

¹²G. Eckart, G. Holzwarth, and J. P. da Providencia, *Nucl. Phys.* **A364**, 1 (1981); H. Koch, G. Eckart, B. Schwesinger, and G. Holzwarth, *ibid.* **A273**, 173 (1982).

¹³C. O. Dorso and E. S. Hernández, *Phys. Rev. C* **26**, 528

(1982).

¹⁴R. Balescu, *Equilibrium and Nonequilibrium Statistical Mechanics* (Wiley, New York, 1975).

¹⁵C. O. Dorso and E. S. Hernández, *Phys. Rev. C* **29**, 1523 (1984).

¹⁶A. S. Jensen, J. Leffers, K. Reese, H. Hofman, and P. J. Siemens, *Phys. Lett.* **117B**, 5 (1982); **117B**, 157 (1982).

¹⁷H. Hoffmann and P. J. Siemens, *Nucl. Phys.* **A257**, 165 (1976).

¹⁸H. Hoffmann and P. J. Siemens, *Nucl. Phys.* **A275**, 464 (1977).

¹⁹C. O. Dorso and E. S. Hernández, *Nucl. Phys.* **A372**, 215 (1982); E. S. Hernández and C. O. Dorso, *ibid.* **A399**, 181 (1983).

²⁰D. Vautherin and D. M. Brink, *Phys. Rev. C* **5**, 626 (1972).

²¹B. L. Berman and S. C. Fultz, *Rev. Mod. Phys.* **47**, 713 (1975); B. L. Berman, *At. Data Nucl. Data Tables* **15**, 319 (1975).

²²R. A. Broglia, in *Nuclear Theory 81*, edited by G. F. Bertsch (World Scientific, Singapore, 1981).

²³M. Danos and W. Greiner, *Phys. Rev.* **138**, B876 (1965).

²⁴C. B. Dover, R. H. Lemmer, and F. J. W. Hahne, *Ann. Phys. (N.Y.)* **70**, 458 (1972).

²⁵C. Yannouleas, M. Dworzecka, and J. J. Griffin, *Nucl. Phys.* **A379**, 256 (1982).

²⁶C. Yannouleas, M. Dworzecka, and J. J. Griffin, *Nucl. Phys.* **A397**, 239 (1983).

²⁷D. Pines and P. Nozieres, *The Theory of Quantum Liquids* (Benjamin, New York, 1966).